PROCEEDINGS, Twenty-First Workshop on Geothermal Reservoir Engineering
Stanford University, Stanford, California, January 27-29, 1997
SGP-TR-155

UPSTREAMING MIMICS CAPILLARITY IN GEOTHERMAL HEAT PIPES

Mark McGuinness

Mathematics Department
Victoria University of Wellington
New Zealand

ABSTRACT

The numerical technique called upstream differencing, applied to mobility terms in Darcy's law for steam and liquid flow in the geothermal simulators TOUGH and MULKOM, is shown to lead to numerical boundary layers in the equations for steady vertical steam-liquid counterflow. These boundary layers are found to be very narrow, and to act in the same way as capillary boundary layers, providing reassurance that upstreaming acts to mimic the physical effect of capillarity.

INTRODUCTION

In a geothermal reservoir, the term heat pipe refers to the steady balanced counterflow of steam and liquid, usually with steam flowing up and liquid flowing down through the same porous medium, so that the net mass flux is small or zero, and there is net heat flux due to the larger specific heat of steam.

Such a heat pipe can form part of the conceptual, mathematical or computer model of a geothermal reservoir, and was first raised in a geothermal context by White *et al* (1971), modelling the Geysers steam field. Gravity is the most important driving force, in contrast to the engineering context, where heat pipes are usually shorter, with heat being moved sideways or downwards against gravity, and capillary effects are important.

Simple modeling of the gravity-driven geothermal heat pipe shows that there are two possible heat pipes for a given heat flux, one vapor-dominated and the other liquid-dominated.

However, including capillary pressure effects into geothermal heat pipes is known *to* lead to narrow capillary boundary layers (McGuinness, 1996, 1997). In these layers, saturation varies rapidly, and changes in capillary pressure are an important mechanism for driving heat flow. Selection of the vapor-dominated or liquid-dominated simple model solution by choice of boundary conditions is a consequence of the capillary boundary layers, so that despite their relatively small vertical extent, they are an important feature of solutions.

A puzzle arising out of this work has been that even in the absence of capillarity, numerical simulations display a qualitatively similar process of solution selection depending on boundary conditions. Earlier work (McGuinness *et al*, 1993) considers the effect on numerical solutions of upstreaming as introducing an iterated map, which explains the selection of one of the simple model solutions, depending on boundary conditions imposed, in a manner analogous to capillarity. However, the relationship between this phenomenon and the effect of capillarity is not clear from that analysis, which also cannot cope with varying the degree of upstreaming, or with calculating the vertical extent of numerical boundary layers. In the present study, the effect of upstreaming is approximated using Taylor's expansion to obtain a differential equation for saturation, allowing direct comparison with capillary effects.

First the simple model is presented, then the effect of upstreaming is added to the model. The effect of adding capillarity to the simple model is compared, and the approximate thickness of the numerical boundary layers arising from upstreaming is calculated. Computer simulations conducted in order to check these results are briefly reported.

Conduction effects are ignored here to simplify the analysis and presentation. Upstreaming continues to mimic capillarity when conduction is included.

STEADY-STATE EQUATIONS

A simple model for the steady vertical counterflow of steam and liquid in a porous medium with conduction and capillary effects excluded is described by the following equations for conservation of mass and energy:

$$u_l + u_v = 0, \quad (1)$$

$$u_l h_l + u_v h_v = Q\,. \quad (2)$$

Subscripts v and l refer to vapor and liquid phases respectively. Q is the heat flux (W/m^2) and h is specific enthalpy (J/kg). When gravity acts in the opposite direction to the vertical coordinate z, Darcy's law for the mass flux density u of each phase in a porous medium is

$$u_l = -\frac{kk_{rl}}{\nu_l}\left(\frac{dP}{dz} + \rho_l g\right), \quad (3)$$

$$u_v = -\frac{kk_{rv}}{\nu_v}\left(\frac{dP}{dz} + \rho_v g\right), \quad (4)$$

where k is the absolute permeability (m^2), k_{rl} is the relative permeability for liquid, k_{rv} is the relative permeability for vapor, ρ is specific density (kg/m^3), g is the gravitational acceleration, and ν is kinematic viscosity (m^2/s). Pressure P and temperature T are monotonically related by the Clausius-Clapeyron equation for steam and liquid in thermodynamic equilibrium,

$$\frac{dT}{dP} = \frac{(T + 273.15)(\rho_l - \rho_v)}{h_{vl}\rho_l\rho_v} \quad (5)$$

The relative permeabilities k_{rv} and k_{rl} depend on the liquid saturation S, and model the choking effect that the presence of vapor has on liquid flow and vice-versa. The fundamental thermodynamic quantities that these equations depend on are chosen to be P and S. Occasionally T will be used in place of P in figures, as it is simply related through the Clausius-Clapeyron equation.

Equations *(1)* and *(2)* represent steady conservation equations that have been integrated once in z, using the two boundary conditions of constant heat flow Q and zero net mass flux. They may be rearranged to obtain

$$\frac{dP}{dz} = \frac{-g(\lambda_l\rho_l + \lambda_v\rho_v)}{\lambda_l + \lambda_v}, \quad (6)$$

$$0 = g\lambda_v(\rho_l - \rho_v) - \frac{Q}{h_{vl}\lambda_l}(\lambda_l + \lambda_v), \quad (7)$$

where the mobilities are $\lambda_l \equiv kk_{rl}/\nu_l$ and $\lambda_v \equiv kk_{rv}/\nu_v$.

Equation *(6)* is a nonlinear first-order differential equation for pressure, coupled with the algebraic condition (7) implicitly relating P and S. Since the right-hand side of equation *(6)* is always negative, it simply says that pressure increases with depth ($-z$). This is a differential algebraic system requiring just one more boundary condition (initial condition in z) to solve. In the usual computer model of a one-dimensional counterflow system it is necessary to impose two more boundary conditions, for example heat and mass fluxes or pressure and saturation at one end. Hence this system of equations is over-determined as it stands, and most boundary conditions will not have solutions, since they do not satisfy the algebraic condition *(7)*.

Condition *(7)* may be plotted as curves relating T and S, for various positive Q/k, as in Fig. 1. Linear relative permeabilities $k_{rl} = S$ and $k_{rv} = 1 - S$ have been used for the purpose of illustration. Note that at a given T and Q/k, there are typically two distinct possible liquid saturation values. The wetter one is termed liquid-dominated, and the drier one is termed vapor-dominated. Solutions to this model must plot along these curves. For the purposes of identification, they will be called ***simple*** model solutions, to distinguish them from two other models, one with upstreaming and one with capillarity effects included.

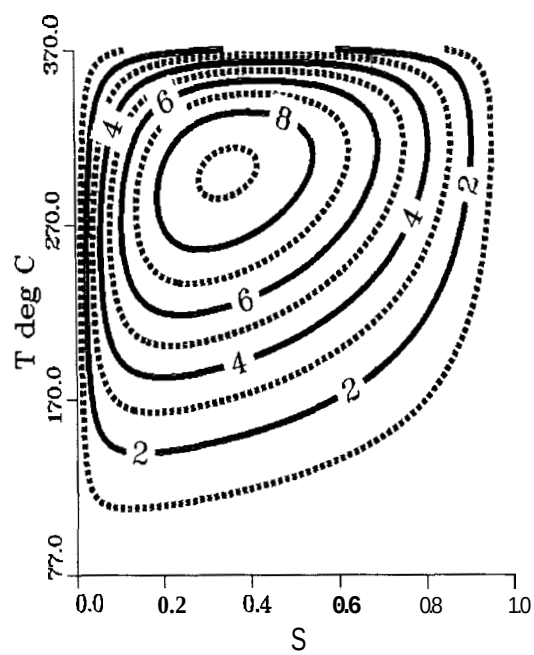

Figure 1. Simple model solution curves, plotted as T vs S, for various values of Q/k in kW/d/m^2.

Upstream Differencing

TOUGH (Transport of Unsaturated Groundwater and Heat) is a multi-dimensional numerical model for simulating the coupled transport of liquid water, vapour, air and heat in porous and fractured media (Pruess, *1988)*. An outgrowth of the simulation package MULKOM, it solves the conservation of mass and energy equations with Darcy's law, with the thermophysical properties of liquid and vapor accurate within experimental uncertainties (Sato *et al*, *1967)*. An integral finite difference

nethod is used for the spatial dependencies, and time-tepping is fully implicit for stability. Volume averages ›ver elements are taken, and placed at a chosen loca-ion in the computation element. In this study, we take his location to be at the center of the element.

A steady-state is obtained by setting up a time-lependent problem, and running it until it is taking ery large time steps and there are no changes in state.

Spatial discretization involves approximating deriva-ives by differences, and taking averages of parame-ers. Different weighting procedures are used for dif-erent parameters (Pruess and Narasimhan, 1985), and ve focus in particular here on the effect on the possi-ble steady-states of upstream differencing, also called ipstreaming. Full upstreaming might be called an ex-reme method, as it uses a value from only one side of he interface instead of taking an average across the in-erface. In TOUGH and MULKOM (and TOUGH2), ipstream differencing is applied to each phase sepa-ately, when calculating the mass flux density using Darcy's law. The mobilities λ_l and λ_v are upstreamed — in the default full upstreaming, the mobility used at he interface is the value obtained from the element up-stream of the interface. This is a technique commonly ised in single-phaseconvection-diffusionproblems for easons of computational economy and stability (eg Raithby, 1976).

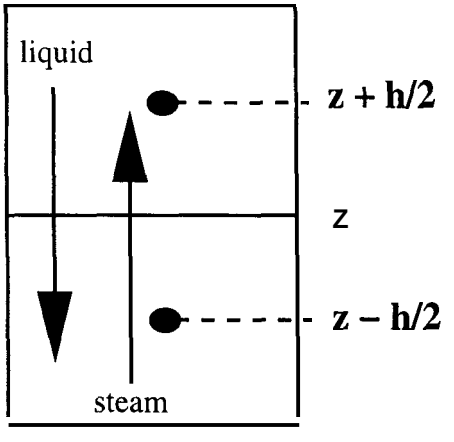

Figure 2. A sketch showing element geometry and notation for upstreaming.

Referring to Fig. 2, when there is a balanced counter-flow, with steam going up and liquid flowing down, full upstreaming means that the mobilities actually used at the interface located at z between two computational elements with centers a distance h apart will be $\lambda_v(z-h/2)$ and $\lambda_l(z+h/2)$. Theparameteraisused to indicate the degree of upstreaming, a = 1being full upstreaming, $a = 1/2$ being central differencing and a = 0 being full downstreaming.

In the appendix, the mobilities are rewritten in terms of their true values at the interface, using Taylor's expansion, and these modified mobilities are substitutedback into the steady-state equations (1) and (2). Some manipulation is required to obtain consistent and explicit differentialequations. To leadingorder in h the following steady-state equations incorporating upstreaming are obtained:

$$\frac{dP}{dz} = -\frac{\frac{Q}{h_{vl}}H_1 + gH_2}{H_3}, \quad (8)$$

$$\epsilon\frac{dS}{dz} = \frac{k_{rl}k_{rv}\left[g\lambda_v\Delta\rho - \frac{Q}{h_{vl}\lambda_l}(\lambda_l+\lambda_v)\right]}{H_3}, \quad (9)$$

where

$$\epsilon \equiv \frac{h}{2}(1-2a)\frac{Q}{h_{vl}\lambda_l}, \quad (10)$$

and

$$H_1 \equiv (k_{rl}k_{rv})', \quad (11)$$

$$H_2 \equiv \left(\lambda_v\rho_v k_{rv}k'_{rl} - \lambda_l\rho_l k_{rl}k'_{rv}\right), \quad (12)$$

$$H_3 \equiv \lambda_v k_{rv}k'_{rl} - \lambda_l k_{rl}k'_{rv} \quad (13)$$

$$\Delta\rho \equiv \rho_l - \rho_v \quad (14)$$

The steady-state equations are now two coupled first-order nonlinear ordinary differential equations, with solutions that are naturally viewed in the phase plane P (or T vs S).

Capillary Effects

When surface tension or capillary pressure is included in the model, the pressures in the liquid and vapour phases are different. Darcy's law becomes (as in McGuinness, 1996, and following Satik *et al,* 1991)

$$u_l = -\frac{kk_{rl}}{\nu_l}\left(\frac{\partial P_l}{\partial z} + \rho_l g\right) \quad (15)$$

$$u_v = -\frac{kk_{rv}}{\nu_v}\left(\frac{\partial P_v}{\partial z} + \rho_v g\right). \quad (16)$$

Capillary pressure is taken to be

$$P_c(S,T) = P_v - P_l, \quad (17)$$

and the particular form for P_c is kept general at this point. Vapor-pressure lowering (the Kelvin effect) is also represented in a general way **as** (after Edlefsen and Anderson, 1948)

$$P_v = f_{\mathrm{vpl}}(T,S)\ P_{\mathrm{sat}}(T) \quad (18)$$

where the vapor-pressure lowering factor is approximated by

$$f_{vpl} = \exp\left\{\frac{-m_l P_c(S,T)}{\rho_l \mathrm{R}(T+273.15)}\right\}, \qquad (19)$$

and where P_{sat} is the saturated vapor pressure of bulk liquid, obeying the Clausius-Clapeyron relation *(5)*.

The dependence of capillary pressure on liquid saturation leads to an extra saturation derivative in the steady-state equations, in a manner analogous to the effect of upstreaming. Substituting these forms for the Darcy velocities into the steady-state equations (1) and (2) and re-arranging terms, the steady-state equations become

$$\frac{dP_v}{dz} = -\frac{Q}{h_{vl}\lambda_v} - g\rho_v , \qquad (20)$$

$$\frac{dP_c}{dS}\frac{dS}{dz} = \frac{g\lambda_v\Delta\rho - \frac{Q}{h_{vl}\lambda_l}(\lambda_l W_1 + \lambda_v)}{\lambda_v W_2} , \qquad (21)$$

where

$$W_1 \equiv 1 - \frac{\partial P_c}{\partial P_v} , \qquad (22)$$

$$W_2 \equiv 1 + \frac{\frac{\partial P_c}{\partial T}\frac{\partial T}{\partial S}}{\frac{\partial P_c}{\partial S}} \qquad (23)$$

W_1 and W_2 are close to 1 in value

MODEL COMPARISON

Including upstreaming or capillarity appears to have dramatically changed the governing equations, not only by replacing the algebraic condition (7) with a differential equation for S, but also by apparently changing the pressure gradient. However, the simple model steady-state equations obtained in the absence of either capillarity or upstreaming have been shown to be a singular limit of the steady-state equations obtained when capillarity is included (McGuinness, 1996,1997). When the term multiplying the saturation derivative is small, it has been shown that steady solutions to the capillary model typically move rapidly through capillary boundary layers, then track the simple model solutions. This gives a system that is no longer overdetermined, and is the usual behaviour of inner and outer solutions to singular perturbation problems. If capillarity is reduced to zero, the boundary layers become narrower, reducing to zero thickness.

Since upstreaming has here been shown to give steady equations of the same form as the capillary model equations, similar results hold. In particular, if ϵ is small, numerical solutions will move rapidly through numerical boundary layers, then track the simple model solutions. These numerical boundary layers have the same orientation or sense as the capillary boundary layers, since both ϵ and $\partial P_c/\partial S$ are negative, provided a > 0.5 (so that mobilities are upstreamed, not downstreamed). Hence upstreaming has qualitatively the same effect as the physical mechanism of capillarity. However, in general the thickness of the numerical boundary layers will be different to the thickness of the capillary boundary layers.

The pressure gradients (6), (40) and (20) look different, but if the algebraic condition (7) is imposed, both the upstreaming and the capillary model pressure gradients reduce exactly to the pressure gradient obtained in the simple model. That is, along the simple solution curves, all models presented here have the same pressure gradients.

Boundary Layer Thickness

The thickness δ of the numerical boundary layers may be estimated by rescaling equation (9). Away from the simple model solutions, the right-hand side of equation (9) has a size of order $g\rho$, or 10^3. Rescaling to $z^* = z/h$, so that distances are now in units of the element size h, equation (9) becomes

$$\epsilon dS = O(10^3 h)dz^* , \qquad (24)$$

so that a change in saturation of order 1 occurs in a distance z^* of order

$$\delta = |\epsilon/(10^3 h)| = \left|\frac{(1-2a)Q}{2h_{vl}\lambda_l 10^3}\right| . \qquad (25)$$

Using typical values $h_{vl} = 10^6$ and $\lambda_l = 10^7 k$, this gives the approximate numerical boundary layer width as

$$\delta = \left|\frac{(1-2a)Q}{2k}\right| \times 10^{-16} . \qquad (26)$$

For balanced counterflow, **Q/k** may take values in the range 10^9–10^{16} W/m^4 (McGuinness, 1996), so that for full upstreaming (a = 1) the boundary layer thickness is in the range 10^{-7}–1 elements. That is, numerical solutions will typically move onto the simple model solutions within one computational element.

NUMERICAL SIMULATIONS

The theoretical result that the numerical boundary layers are typically less than one element in size has been verified by numerical simulations using TOUGH2. In order to verify the detailed structure of the expression (26) for boundary layer thickness, it is useful to consider a non-typical heat pipe, with a boundary layer that is everywhere very close to the simple solutions, so

hat the right-hand side of equation (9) is close to zero, nstead of being of order 10^3. This occurs when heat low is raised to near the maximum value it may take, bout $10^{16}k$ W, when a vapor-dominated heat pipe is nade to overly a liquid-dominated heat pipe. Then the iumerical boundary layer thickness is observed in simlations to increase to several tens of elements, and the ffects of changing the value of the upstreaming factor , the element size h, and Q/k, may be seen.

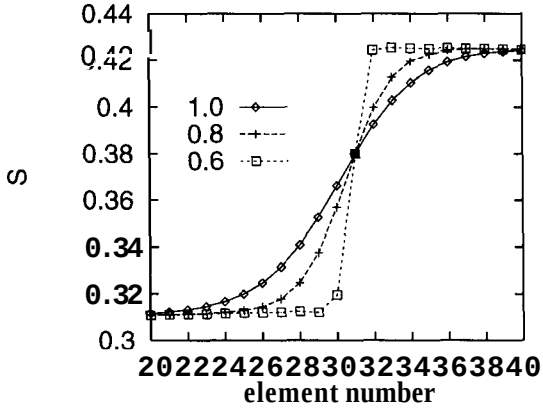

Figure 3. The effect of varying the upstreaming factor a, on numerical boundary layers. Each different line is For a different value of a.

δ/h	a	$\delta/(2a-1)$
20 ± 4	1.0	20 ± 4
10 ± 2	0.8	17 ± 4
3 ± 1	0.6	15 ± 5

Table 1. Numerical boundary layer thickness 6 against upstreaming a.

A 1D vertical balanced counterflow was set up with $Q = 8.7$ kW/m^2, $k = 1$d, and 60 computational elements each about 1m long. **A** large volume element was used in the middle of the heat pipe, with temperature held at 310°C and liquid saturation held at 0.38. The simulations was allowed to run until the heat pipe stabilised to a steady-state at each value of upstreaming used, with a liquid-dominated heat pipe below the large element, and a vapor-dominated heat pipe above the large element, connected across a numerical boundary layer. The width of this boundary layer was found to vary as predicted by the above analysis, getting thicker as the upstreaming factor a was changed from 1 down to near 0.5. Values of saturation obtained from TOUGH2 simulations are plotted against element number in Fig. 3. Boundary layer thickness was estimated by looking at these, and is tabulated in Table 1. Note that the thickness does appear to be approximately proportional to 2a-1.

When upstreaming is close to 0.5 (central differencing), the heat pipe will not stabilize, and elements appear to alternate between the vapor and the liquid-dominated simple curves.

When permeability is changed, but Q/k is held constant, there is no visible change in simulation solutions. When element size is changed, the numerical boundary layer changes proportionally, as seen in Fig. 4. Since S is plotted here against element number, no change is seen in the boundary layer. Some changes are visible away from the boundary layer, due to the change in vertical scale.

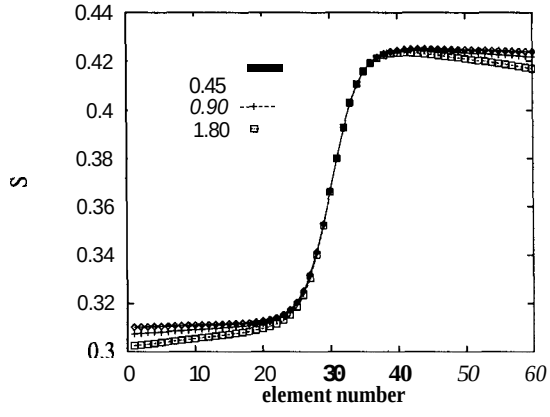

Figure 4. The effect of varying the element size h (m), on numerical boundary layers.

CONCLUSIONS

Upstreaming, when applied to vertical steam-liquid counterflow, acts to mimic the physical mechanism of capillarity in a qualitative way. The results for capillary effects discussed in McGuinness (1996,1997)then apply to numerical simulations even in the absence of capillarity, with the proviso that the thickness of the numerical boundary layers will be different to that of the capillary boundary layers.

This is a reassuring result for users of the geothermal simulators TOUGH and MULKOM, and helps to understand the process **of** selection of either the vapor-dominated or the liquid-dominated simple model steady-state that occurs depending on the boundary conditions imposed in simulations.

In particular, upstreaming leads to narrow boundary layers, typically much less than one computational element in size. Upstreaming makes the simple steady-state model well-posed, as the number of boundary

onditions is now correct, so that steady solutions exist n general. The easiest way to set up a steady heat ipe with a specified heat flux is to impose the heat lux and zero mass flux at one end, and to impose contant pressure and saturation at the other end with a arge-volume computation element. **A** heat pipe with i large element at the top will typically converge to he liquid-dominated solution, and a heat pipe with a arge element at the bottom will typically converge to he vapor-dominated solution.

ICKNOWLEDGEMENTS

Numerical simulations were performed on computer :quipment funded by the New Zealand Lotteries Grants Board and the Internal Grants Committee of Victoria Jniversity of New Zealand. I am grateful to Steve White for suggestions that showed the way forward n this work; and to Roger Young, Warwick Kissling and Karsten Pruess for their generosity with various software.

REFERENCES

V.E. Edlefsen, and A.B.C. Anderson (1948) Thermodynamics of Soil Moisture, *Hilgardia,* **15** No.2, 231-298.

M.C. Leverett (1941) Capillary behaviour in porous solids, *AIME Trans.* **142,** 52.

M.J. McGuinness (1996) Steady solution selection and existence in geothermal heat pipes. I: the convective case, *Int. J. Heat and Mass Transfer;* 39 No. 2, 259–274.

M.J. McGuinness (1997), Steady solution selection and existence in geothermal heat pipes. **11:** the conductive case, *Int. J. Heat and Mass Transfer,* 40 No. 2, 311–321.

M.J. McGuinness, M. Blakeley, K. Pruess, and M.J. O'Sullivan (1993) Geothermal Heat Pipe Stability: Solution Selection by Upstreaming and Boundary Conditions, *Transport in Porous Media* **11,** 71–100.

K. Pruess (1988), SHAFT, MULKOM, TOUGH: a set of numerical simulators for multiphase fluid and heat flow, *Geotermia, Rev. Mex. Geoenergia* **4** (1), 185–202.

K. Pruess and T.N. Narasimhan (1985) A practical method for modeling fluid and heat flow in fractured porous media, *Soc. Petroleum Eng. J.* **25** No.1, 14–26.

G.D. Raithby (1976), A critical evaluation of upstream differencing applied to problems involving fluid flow, *Comp. Methods in Appl. Mechs. and Eng.* **9**, 75–103.

T. Sato, T. Minamiyama and J. Yata (1967), A formulation of the thermodynamic properties of ordinary water substance, *Kyoto University Faculty of Engineering Memoirs,* 29 Part 1, 16–27.

C. Satik, M. Parlar, and Y.C. Yortsos (1991), **A** Study of Steady-state Steam-water Counterflow in Porous Media, *Int. J. Heat and Mass Transfer,* **34** No.7, 1755–1772.

D.E. White, J.P. Muffler and A.H. Truesdell (1971) Vapor-dominated hydrothermal systems compared with hot-water systems, *Econ. Geology* **64**, 75–97.

APPENDIX

Here are the details of the derivation of the upstreaming steady-state equations. Referring to Fig. 2, the mobilities actually used at the interface z are

$$\lambda_l = a\lambda_l(z+h/2) + (1-a)\lambda_l(z-h/2), \tag{27}$$

$$\lambda_v = a\lambda_v(z-h/2) + (1-a)\lambda_v(z+h/2). \tag{28}$$

Use of the Taylor series allows us to relate these values to the true values at the interface,

$$\lambda_l(z+h/2) = \lambda_l(z) + \frac{h}{2}\frac{d\lambda_l}{dz} + O(h^2), \tag{29}$$

$$\lambda_v(z-h/2) = \lambda_v(z) - \frac{h}{2}\frac{d\lambda_v}{dz} + O(h^2). \tag{30}$$

Derivatives are to be evaluated at the interface z. The notation $O(h^2)$ indicates that terms of size h^2 have been neglected. In this paper, k is constant. Viscosity depends on z through P, and relative permeabilities depend on z through S. Hence by the chain rule,

$$\frac{d\lambda_l}{dz} = \frac{k}{\nu_l}\frac{dk_{rl}}{dS}\frac{dS}{dz} - \frac{kk_{rl}}{\nu_l^2}\frac{d\nu_l}{dP}\frac{dP}{dz}, \tag{31}$$

ınd a similar equation holds for λ_v. Taking equations (3) and (4) at the interface z, and replacing the mobilities with he upstreamed mobilities gives

$$u_l = -\left[\lambda_l + (2a-1)\frac{h}{2}\frac{k}{\nu_l}\left(k'_{rl}\frac{dS}{dz} - \frac{k_{rl}}{\nu_l}\nu'_l\frac{dP}{dz}\right) + O(h^2)\right]\left(\frac{dP}{dz} + \rho_l g\right), \tag{32}$$

$$u_v = -\left[\lambda_v - (2a-1)\frac{h}{2}\frac{k}{\nu_v}\left(k'_{rv}\frac{dS}{dz} - \frac{k_{rv}}{\nu_v}\nu'_v\frac{dP}{dz}\right) + O(h^2)\right]\left(\frac{dP}{dz} + \rho_v g\right) \tag{33}$$

All expressions are evaluated at the interface z in equations (32) and (33). Upstreaming has led to new terms in these equations involving $\frac{dS}{dz}$, $\frac{dS}{dz}\frac{dP}{dz}$ and $(\frac{dP}{dz})^2$, corresponding to the *false diffusion* studied in Raithby (1976). .

The new term with $\frac{dS}{dz}$ is of particular interest, and represents a structural change in the equations. Such an extra derivative is usually associated with boundary layers in singular perturbation theory. The governing steady-state equations (1) and (2) become

$$\left[\lambda_l + (2a-1)\frac{h}{2}\frac{k}{\nu_l}\left(k'_{rl}\frac{dS}{dz} - \frac{k_{rl}}{\nu_l}\nu'_l\frac{dP}{dz}\right)\right]\left(\frac{dP}{dz} + \rho_l g\right) +$$
$$\left[\lambda_v - (2a-1)\frac{h}{2}\frac{k}{\nu_v}\left(k'_{rv}\frac{dS}{dz} - \frac{k_{rv}}{\nu_v}\nu'_v\frac{dP}{dz}\right)\right]\left(\frac{dP}{dz} + \rho_v g\right) = O(h^2), \tag{34}$$

$$\left[\lambda_v - (2a-1)\frac{h}{2}\frac{k}{\nu_v}\left(k'_{rv}\frac{dS}{dz} - \frac{k_{rv}}{\nu_v}\nu'_v\frac{dP}{dz}\right)\right]\left(\frac{dP}{dz} + \rho_v g\right)h_{vl} = -Q + O(h^2) \tag{35}$$

These equations are not explicit in the derivatives as they stand. In fact, terms of order h^2 are not consistently neglected. This can be rectified by noting that equation (35) can be written either in the form

$$\frac{dP}{dz} + \rho_v g = \frac{-Q}{\lambda_v h_{vl}} + O(h), \tag{36}$$

or in the form

$$\frac{dP}{dz} + \rho_l g = \frac{Q}{\lambda_l h_{vl}} + O(h), \tag{37}$$

Substituting these into the terms which are nonlinear in the derivatives in equations (34) and (35) then gives conservation equations that are consistent to order h^2 and explicit in the derivative terms,

$$\left[\lambda_l + \lambda_v - \frac{h}{2}(2a-1)\frac{Q}{h_{vl}}\left(\frac{\nu'_l}{\nu_l} + \frac{\nu'_v}{\nu_v}\right)\right]\frac{dP}{dz} +$$
$$\frac{h}{2}(2a-1)\frac{Q}{h_{vl}}\left(\frac{k'_{rl}}{k_{rl}} + \frac{k'_{rv}}{k_{rv}}\right)\frac{dS}{dz} = -g(\lambda_l\rho_l + \lambda_v\rho_v), \tag{38}$$

$$\left[\lambda_v - \frac{h}{2}(2a-1)\frac{Q}{h_{vl}}\frac{\nu'_v}{\nu_v}\right]\frac{dP}{dz} + \frac{h}{2}(2a-1)\frac{Q}{h_{vl}}\frac{k'_{rv}}{k_{rv}}\frac{dS}{dz} = \frac{-Q}{h_{vl}} - g\lambda_v\rho_v . \tag{39}$$

If a $= 1/2$ then equations (6) and (7) are recovered, as central differencing is second order in h.

Solving for the gradient terms gives to leading order in h, provided a is not equal to 1/2:

$$\frac{dP}{dz} = \frac{\frac{Q}{h_{vl}}(k_{rl}k_{rv})' + g\left(\lambda_v\rho_v k_{rv}k'_{rl} - \lambda_l\rho_l k_{rl}k'_{rv}\right)}{\lambda_l k_{rl}k'_{rv} - \lambda_v k_{rv}k'_{rl}}, \tag{40}$$

$$\epsilon\frac{dS}{dz} = \frac{k_{rl}k_{rv}\left[g\lambda_v(\rho_l - \rho_v) - \frac{Q}{h_{vl}\lambda_l}(\lambda_l + \lambda_v)\right]}{\lambda_v k_{rv}k'_{rl} - \lambda_l k_{rl}k'_{rv}}, \tag{41}$$

where

$$\epsilon \equiv \frac{h}{2}(1 - 2a)\frac{Q}{h_{vl}\lambda_l} . \tag{42}$$

This choice of ϵ ensures that the terms on the right-hand side of equation (40) are of the same order as terms on the right-hand side of equation (41).